Magneto-Rayleigh-Taylor experiments on a MegaAmpere linear transformer driver

J. C. Zier,[1,a)] R. M. Gilgenbach,[1,b)] D. A. Chalenski,[1] Y. Y. Lau,[1] D. M. French,[1,c)] M. R. Gomez,[1,d)] S. G. Patel,[1] I. M. Rittersdorf,[1] A. M. Steiner,[1] M. Weis,[1] P. Zhang,[1] M. Mazarakis,[2] M. E. Cuneo,[2] and M. Lopez[2]
[1]*Department of Nuclear Engineering and Radiological Sciences, University of Michigan, Ann Arbor, Michigan 48109-2104, USA*
[2]*Sandia National Laboratories, Albuquerque, New Mexico 87185, USA*

(Received 14 December 2011; accepted 27 January 2012; published online 5 March 2012)

Experiments have been performed on a nominal 100 ns rise time, MegaAmpere (MA)-class linear transformer driver to explore the magneto-Rayleigh-Taylor (MRT) instability in planar geometry. Plasma loads consisted of ablated 400 nm-thick, 1 cm-wide aluminum foils located between two parallel-plate return-current electrodes. Plasma acceleration was adjusted by offsetting the position of the foil (cathode) between the anode plates. Diagnostics included double-pulse, sub-ns laser shadowgraphy, and machine current B-dot loops. Experimental growth rates for MRT on both sides of the ablated aluminum plasma slab were comparable for centered-foils. The MRT growth rate was fastest (98 ns e-folding time) for the foil-offset case where there was a larger magnetic field to accelerate the plasma. Other cases showed slower growth rates with e-folding times of about ~106 ns. An interpretation of the experimental data in terms of an analytic MRT model is attempted. © *2012 American Institute of Physics*. [http://dx.doi.org/10.1063/1.3690088]

I. INTRODUCTION

There has been a recent resurgence of interest in imploding liners for magnetized target fusion.[1–8] In the Sandia National Laboratories concept, a magnetically compressed cylindrical liner adiabatically heats and compresses a laser-preionized plasma.[3] The most important concern is that the liner symmetry could be disrupted by the magneto-Rayleigh–Taylor (MRT) instability, in which the light fluid (magnetic field) accelerates the (heavy) liner plasma.[9–12] While this problem was studied by Harris in 1962,[9] that work did not sufficiently distinguish between MRT and RT concerning the crucial issues of anisotropy (due to the magnetic field direction) and feedthrough of the instability between two interacting edges on either side of the heavy material. We have recently developed an ideal magnetohydrodynamic (MHD) theory of MRT on a simple planar geometry model relevant to the present experiments, with emphases on the effects of anisotropy and feedthrough.[13] The theory readily accounts for arbitrary directions of the magnetic field tangential to the interfaces of different regions.[14]

The present paper describes MRT experiments that were performed on a MA-class linear transformer driver (LTD) utilizing a planar geometrical configuration.[15] This simple geometry was easily probed by laser diagnostics and was not subject to the kink instability.

II. EXPERIMENTAL CONFIGURATION

Experiments were performed on the Michigan accelerator for inductive Z-pinch experiments (MAIZE) facility that consisted of an LTD capable of generating a 1 MA drive current at 100 kV across a low-inductance matched load with <100 ns rise time.[16] This machine was designed and initially constructed at the Institute of High Current Electronics in Tomsk, Russia. The LTD transmitted power to the plasma physics experiment by a radial magnetically insulated transmission line (MITL) that transformed to a stripline at the load region as shown in Figs. 1(a) and 1(b).

The load consisted of a 400 nm-thick, 1 cm-wide, Al cathode foil mounted between two parallel-plate anodes that served as return current paths, forming a 1.3-cm-tall interaction region as depicted in Fig. 2. When the foil was centered between the electrodes, theory dictated that there was zero net magnetic pressure, resulting in zero foil acceleration. Small experimental variations in foil location led us to call the 15 shots with this 0.1 ± 0.3 mm initial offset the "small offset" case, which closely simulated the ideal centered-foil conditions. By offsetting the initial position of the foil closer to the left anode plate, i.e., $x_0 < 0$ in Fig. 2, the foil magnetic-pressure differential accelerated the foil center of mass towards the center of the gap. We referred to the 10 shots with this 1.1 ± 0.3 mm initial offset as the "large offset" case. This acceleration of the foil plasma (heavy fluid) by the magnetic field (light fluid) was expected to drive MRT. Experiments were performed comparing the small offset (nearly centered) and large offset foil positions. The LTD was limited to 70% of the maximum charge voltage due to the overmatched nature of this foil load. The primary diagnostic was a two frame, sub-ns Nd:YAG laser shadowgraphy system operated at 532 nm with a 9 ns delay between frames. Current was measured using B-dot monitors.

[a)]Present address: Naval Research Laboratory, Washington, DC 20375, USA
[b)]Author to whom correspondence should be addressed. Electronic mail: rongilg@umich.edu.
[c)]Present address: Air Force Research Laboratory, Kirtland AFB, New Mexico 87117, USA.
[d)]Present address: Sandia National Laboratories, Albuquerque, New Mexico 87185, USA.

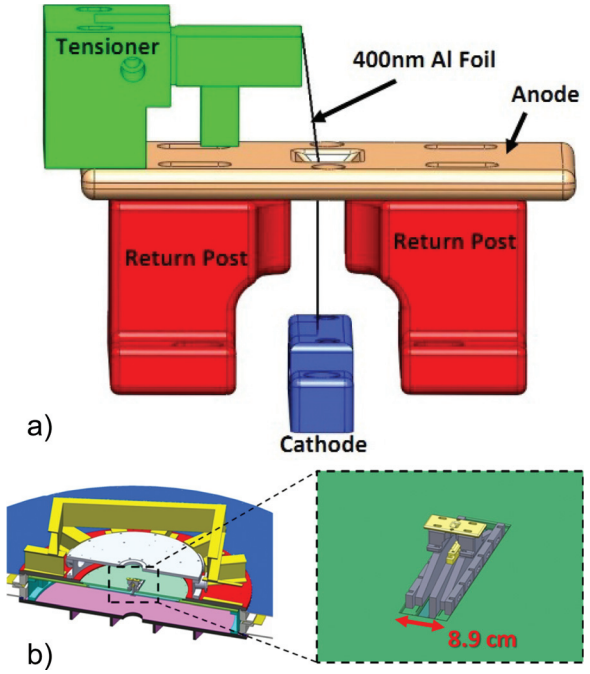

FIG. 1. (Color) CAD renderings of (a) the load assembly and (b) the transmission line/vacuum hardware. The tensioning system is removed from (b) for clarity.

From the experimental data, this simple picture of a thin aluminum foil was significantly modified after the foil was ablated into an aluminum plasma slab, which had a much greater thickness, of order 1 mm and beyond. According to our MRT theory, this made the left side and the right side of the plasma slab essentially decoupled.

III. EXPERIMENTAL RESULTS AND DISCUSSION

Experimental current traces are shown in Figs. 3(a) and 3(b) for the two cases of initial foil position: large offset and small offset. The current risetime was on the order of 150 ns, slower than the matched, resistive load risetime due to the inductance of the load and transmission line. For the large offset case, the drive current reproducibility diminished beyond approximately 100 ns into the pulse compared to the small offset case. This difference is a topic of ongoing research, but is believed to be a result of load dynamics given the exceptional reproducibility of the LTD itself.[16]

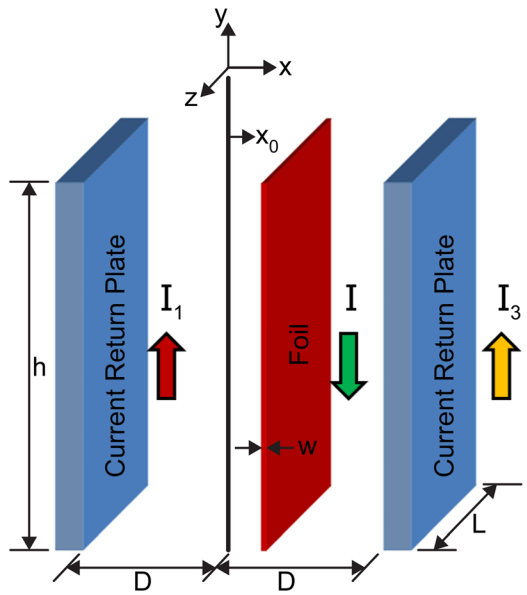

FIG. 2. (Color online) The planar geometry used in development of MRT theory and experimental load design. For the experiment, the large offset case corresponded to the initial foil position $x_0 < 0$, and the small offset case corresponded to the initial foil position $x_0 \approx 0$.

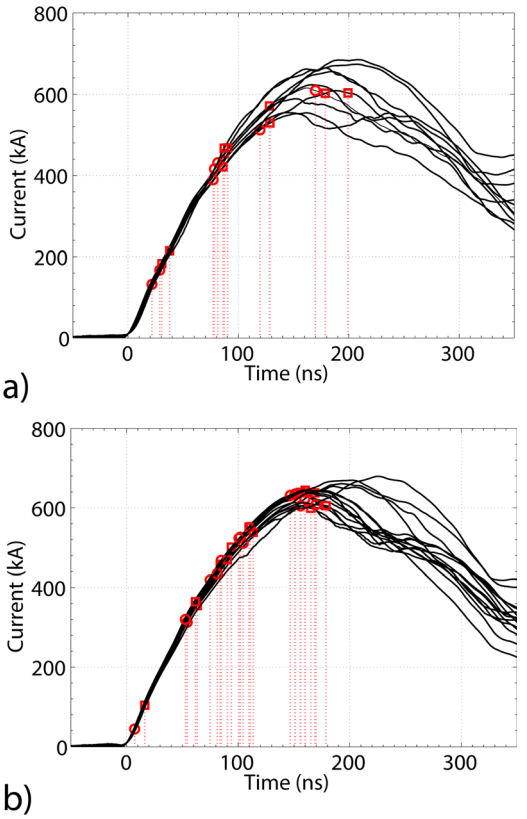

FIG. 3. (Color online) Laser timings and current trace overlays for (a) the large and (b) the small offset cases. Circles indicate an image from camera 1 and squares indicate an image from camera 2, which was delayed 9 ns.

A sample laser shadowgraphy image of an ablated foil at a peak current of 0.6-MA is shown in Fig. 4. Several features were apparent for this foil, which had a large initial offset to the left in the picture,

(1) the foil plasma was accelerated to the right (towards the center),
(2) the instability growth was faster on the left side (expected to be MRT unstable),
(3) the instability was also apparent on the right side, due to the deceleration of the rightward expansion of the plasma plume. This deceleration resulted from the rising magnetic pressure to the right of the plasma slab during the current risetime.

Early time shadowgraphy images, as in Fig. 5(a), have shown that the MRT was seeded by what was believed to be the electrothermal instability (ET)[12,17]. A time sequence over four shots in Figs. 5(a)–5(d) shows how the instability grew over time.

The shadowgraphy images for both cases were analyzed by a computer algorithm and a figure of merit was calculated

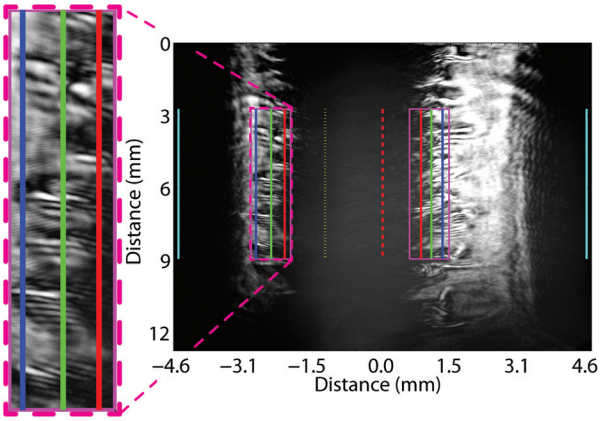

FIG. 4. (Color) A sample laser shadowgraphy image at peak current for the large offset case, shot 301 at 199 ns and 603 kA, showing the region-of-interest used for the MRT growth rate analysis. The dashed yellow line represents the approximate location of pre-shot center of foil. The dashed red line represents the midplane between the original anode plate locations, which are shown in solid cyan. The magenta boxes represent the extents of plasma used in the analysis. The blue (left), green (middle), and red (right) lines within the magnified region-of-interest represent the locations corresponding to 85%, 50%, and 15% laser transmission thresholds, respectively. The figure-of-merit used to characterize the amplitude of the MRT structure was defined as the distance between the 85% and 15% thresholds.

to characterize the amplitude of the surface ripples from MRT growth when a given image was taken.[15] This figure of merit was plotted for both offset cases, and an exponential fit was applied, yielding the average, measured growth rate. The wavelength-spectrum of the instability development was computed from the shadowgraphy data as depicted in Figs. 6(a) and 6(b). The contribution due to the ET instability was seen at early times (Fig. 6(a)) as the short wavelength features at $\lambda = \sim 0.4$ mm. The longer wavelength contribution ($\lambda > 0.7$ mm) developed and grew at later times (Fig. 6(b)) and was attributed to MRT.

Instability growth rate measurements were extracted from the exponential fits, as presented in Figs. 7 and 8. The fastest growth rate of the MRT was expected for the case of maximum plasma acceleration by the magnetic field, which corresponded to the left side of the foil with large offset towards the left-hand return current plate. Data in Fig. 7(a) agreed with this prediction in that the fastest MRT growth rate was observed, with an e-folding time of approximately 98 ns.

For the large offset case, once the rightward expansion of the foil-ablated plasma became retarded by the rising magnetic pressure to the right of the plasma slab, the right side of the plasma slab was also subject to MRT growth. Fig. 7(b) displays the experimentally observed exponential

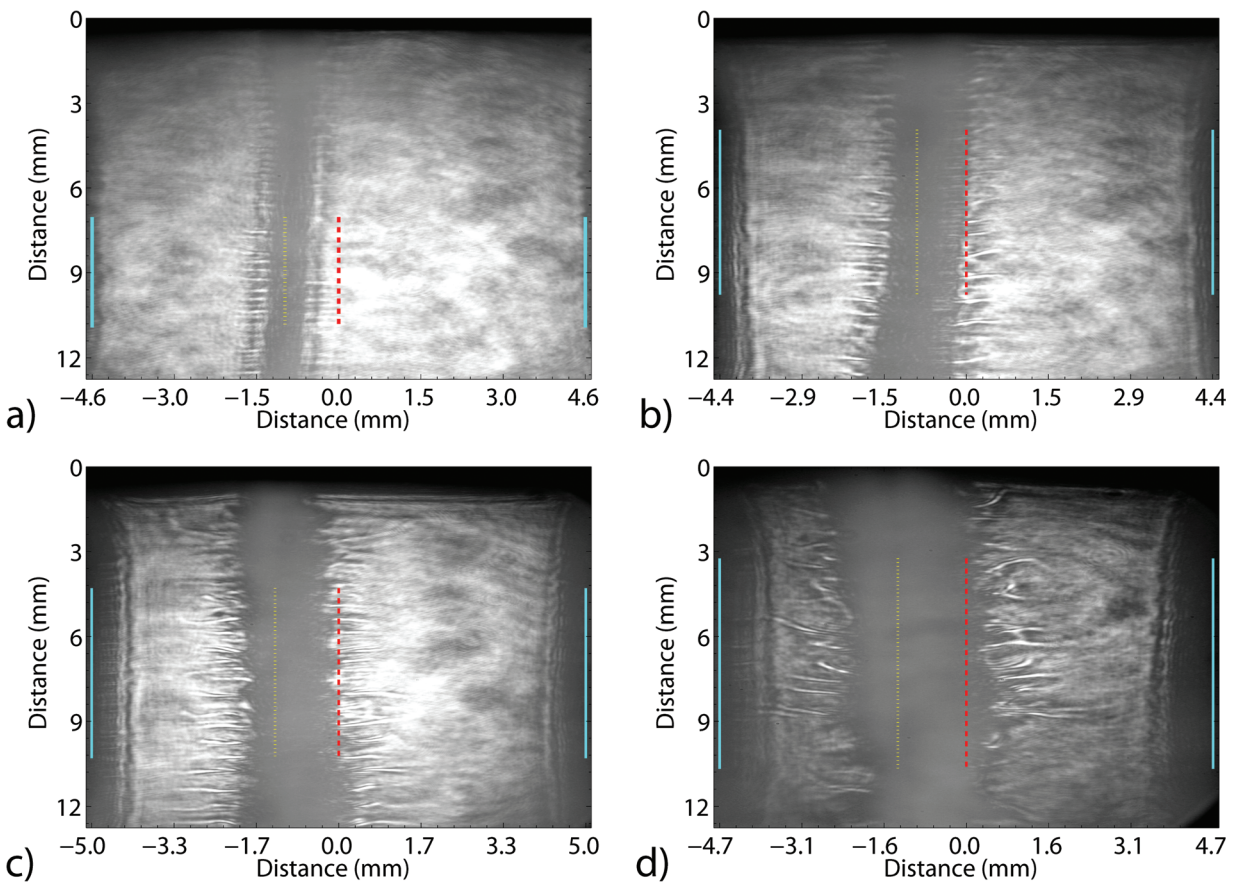

FIG. 5. (Color) A laser shadowgraph image sequence for the large offset case: (a) shot 309 at 38 ns and 215 kA, (b) shot 310 at 90 ns and 468 kA, (c) shot 306 at 129 ns and 529 kA, and (d) shot 337 at 179 ns and 602 kA. The horizontal aspect ratio has been stretched and the contrast enhanced to aid in viewing the instability development. The yellow lines represent the center of the pre-shot foil location, the dashed red line represents the center plane between the return current electrodes, and the solid cyan lines represent the original return current electrode locations.

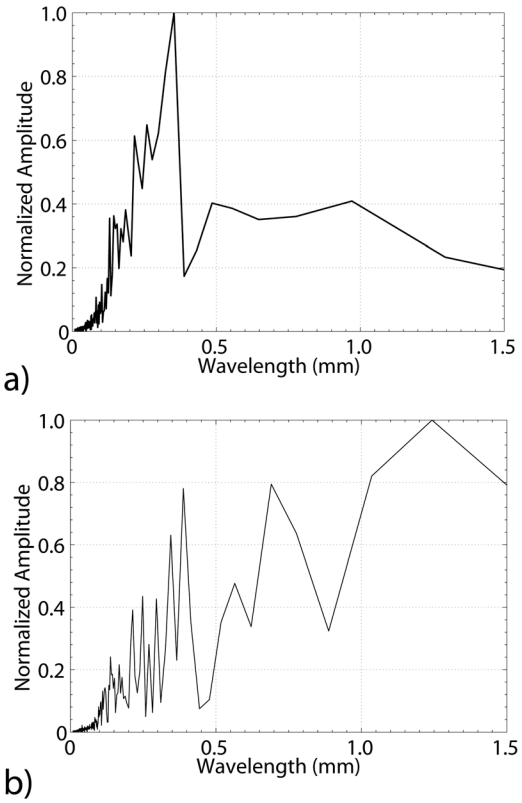

FIG. 6. The wavelength spectra taken from the left interface for the large offset case for (a) shot 309 at 38 ns and 215 kA and (b) shot 301 at 199 ns and 603 kA. The early time spectra (a) is dominated by the short wavelength structure from the ET instability ($\lambda \sim 0.4$ mm), whereas the late time spectra (b) contains the longer wavelength MRT ($\lambda > 0.7$ mm) modulating the shorter wavelength structure.

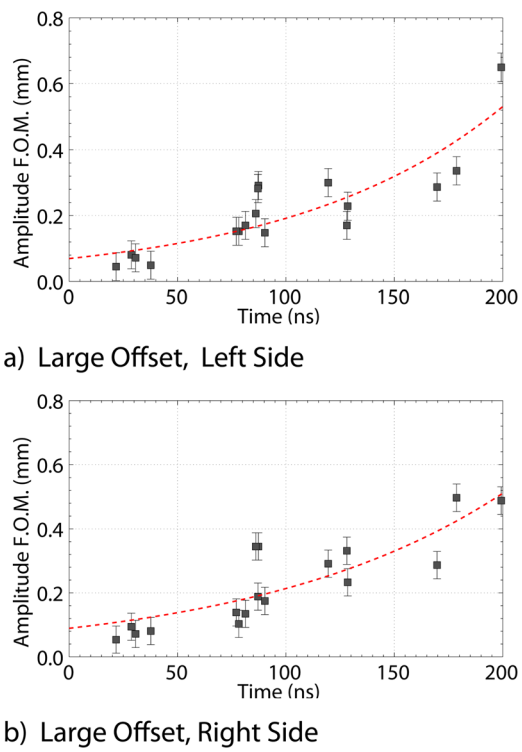

FIG. 7. (Color online) The experimental figure-of-merit measurements characterizing the MRT amplitude for the large offset (a) left side and (b) right side. The red dashed line represents the empirical fit used to determine the average MRT growth rate.

growth of the instability on the right side of the foil plasma with large initial offset, with an e-folding time of approximately 114 ns, a correspondingly lower growth rate than that observed for the left side foil plasma.

For the small offset case, one expects that MRT will grow on both sides of the foil plasma due to the expansion of the plasma. This is similar to the interfaces in the large offset case, but with a smaller MRT growth rate than the left side of the large offset case, because the magnetic pressure on both sides of the small offset case is weaker. This effect was measured in the data, as presented in Figs. 8(a) and 8(b), which showed exponential growth with e-folding times of about 106 ns for the small offset case (both left and right sides). Table I summarizes the experimental measurements of the MRT growth rates for the various cases tested.

A. Interpretation of the experimental data

Our interpretation of the experimental data focused on two aspects of the theory: instability growth rates and the feedthrough factors. The feedthrough factor is dependent upon the normalized product $k\Delta$,[13] with k equal to the instability wave number and Δ equal to the foil/plasma slab thickness. Experiments indicated that the foil thickness rapidly expanded from the initial value of 400 nm to at least 1 mm by 50 ns after start of current and up to 3 mm and larger at later times (Figs. 5(a)–5(d)). Thus, the feedthrough factor of MRT between the left surface and the right surface, $F = e^{-k\Delta}$, was exceedingly small.[9,13] Using $k = 2\pi/(0.8\,\text{mm})$ from Fig. 6(a) and $\Delta = 1$ mm as indicated above, $F = 0.00039$, which is

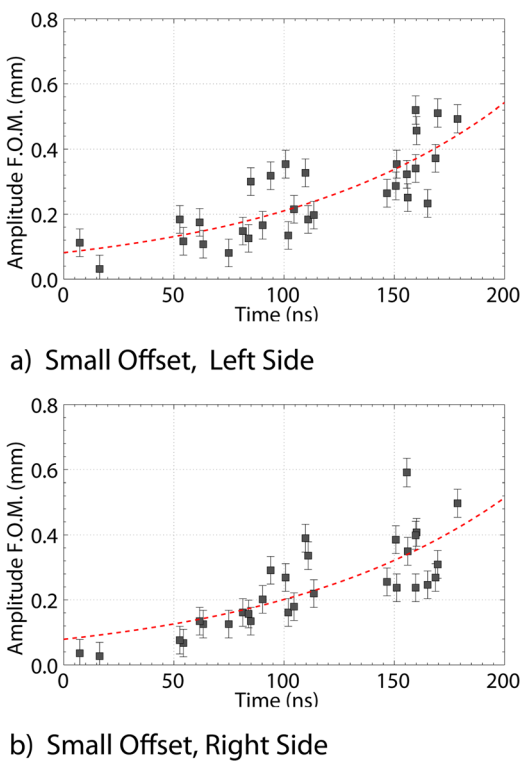

FIG. 8. (Color online) The experimental figure-of-merit measurements characterizing the MRT amplitude for the small offset (a) left side and (b) right side. The red dashed line represents the empirical fit used to determine the average MRT growth rate.

TABLE I. A summary of MRT observations and e-folding times.

Case	Expected fluid configuration	Observed fluid configuration	e-Folding time (ns)
Large offset, left side	"Light" B-field accelerates "heavy" plasma	Highest magnetic pressure drives fastest growth on MRT unstable interface	98 ± 15
Large offset, right side	"Light" B-field decelerates "heavy" plasma	Early expansion allows right side magnetic pressure to produce MRT unstable interfaces after interfaces decouple	114 ± 20
Small offset, left side	No driving acceleration	Both sides show similar growth rate due to early expansion followed by later time magnetic compression	105 ± 17
Small offset, right side	No driving acceleration	Both sides show similar growth rate due to early expansion followed by later time magnetic compression	107 ± 20

much less than unity. This meant that the MRT development of the left surface and the right surface of the ablated plasma slab were completely decoupled. We may then assume that the slab width was infinite when we considered the evolution MRT on the left surface or the right surface, in which case the classical theories of an infinite slab by Kruskal and Schwarzschild[10] and by Chandrasekhar[11] applied. This was true for both large and small offsets because there was rapid expansion of the plasma thickness in both cases.

The next question concerns appreciable MRT growth, with comparable growth rates on the left and right interfaces, regardless of whether the foil has a large or small offset. The underlying reason lies with the x-dependence of the magnetic pressure (Fig. 2). Since the magnetic field, B_z, changed sign across the slab, B_z was zero somewhere inside the slab. That is, the magnetic pressure was minimum at the center of the plasma slab and was maximum at the edges. It then followed that the acceleration, provided by the magnetic pressure gradient, that drove MRT always pointed toward the center of the plasma slab. Therefore, both the left and right edges of the plasma slab were MRT unstable, regardless of the initial offset.

We envision the development of MRT thus. Initially, when the current was low, the foil was ablated and the plasma rapidly expanded. At this early stage, the ET dominated.[12,17] After this initial stage, the current builds up. The magnetic pressure increased, providing retardation of the plasma expansion on *both* sides of the plasma slab. It was this retardation on both sides (i.e., acceleration from the light fluid, the magnetic field, to the heavy fluid, the plasma) that led to MRT on both sides, as explained in the preceding paragraph. The ET seeds the MRT (Fig. 6).

Facing large uncertainties in plasma parameters and the nonlinear evolution of MRT, we use the MRT dispersion relation for the growth rate, γ, of an interface,[9–13]

$$\gamma^2 = (k_y^2 + k_z^2)^{1/2} g - k_z^2 V_A^2, \tag{1}$$

where k_y and k_z are the wavenumbers in the y- and z-directions (Fig. 2) and V_A is the Alfven speed. Since the ET is presumably due to surface roughness and is isotropic on the surface (when the current is low), we postulate that $k_y = k_z$, and Eq. (1) becomes

$$\gamma^2 = \sqrt{2} k_y g - k_y^2 V_A^2. \tag{2}$$

Differentiating Eq. (2) with respect to k_y, we obtain the maximum growth rate, $\gamma = \gamma_m$, occurring at the wavenumber $k_y = k_{ym} = g/(\sqrt{2} V_A^2)$. The last expression gives V_A^2 in terms of g and k_{ym}. Evaluating Eq. (2) at $k_y = k_{ym}$, we obtain the maximum MRT growth rate,

$$\gamma_m^2 = k_{ym} g(\sqrt{2} - 1/\sqrt{2}) = 0.707 k_{ym} g. \tag{3}$$

Equation (3) may be rewritten as,

$$g = \frac{\gamma_m^2}{0.707 k_{ym}} = 2.25 \times \left(\frac{\lambda_m}{1\text{mm}}\right) \times \left(\frac{1}{\tau/(100\text{ ns})}\right)^2 \text{cm}/(\mu\text{s})^2, \tag{4}$$

where $\lambda_m = 2\pi/k_{ym}$ is the wavelength in the y-direction of the most unstable MRT mode, and $\tau = 1/\gamma_m$ is the e-folding time of this growing mode. The last expression in Eq. (4) gives the numerical value.

If we further postulate that the measured MRT growth rates in Figs. 4 and 5 corresponded to the most unstable mode at the interface (left or right), and that the dominant feature in the k_y spectrum (Fig. 6) corresponded to this most unstable mode, we may infer from Eq. (4) what should have been the acceleration, g, at the interface to give rise to such an MRT growth on this interface. From Fig. 6, we take λ_m between 0.8 mm and 1.2 mm. From Sec. II, the measured MRT e-folding times were $\tau = 98$ ns, 114 ns, and ~106 ns, respectively, for large offset left interface, large offset right interface, and small offset (either interface). Substituting these values of λ_m and τ into Eq. (4), we obtain,

$$\begin{aligned} g &= 2.34 \pm 0.47 \text{ cm}/\mu\text{s}^2, \text{large offset, left side} \\ g &= 1.73 \pm 0.35 \text{ cm}/\mu\text{s}^2, \text{large offset, right side} \\ g &= 2.0 \pm 0.4 \text{ cm}/\mu\text{s}^2, \text{small offset, either side} \end{aligned} \tag{5}$$

TABLE II. A direct measurement of the interface accelerations for laser transmission threshold locations as illustrated in Fig. 4.

Location	Large offset left side (cm/μs²)	Large offset right side (cm/μs²)	Small offset left side (cm/μs²)	Small offset right side (cm/μs²)
15%	6.6 ± 3.5	1.9 ± 2.6	2.3 ± 2.9	−2.8 ± 2.3
Mean	6.5 ± 3.5	1.2 ± 2.4	3.9 ± 3.0	−5.3 ± 2.3
85%	7.2 ± 3.6	−0.5 ± 2.5	4.6 ± 3.2	−5.8 ± 2.8

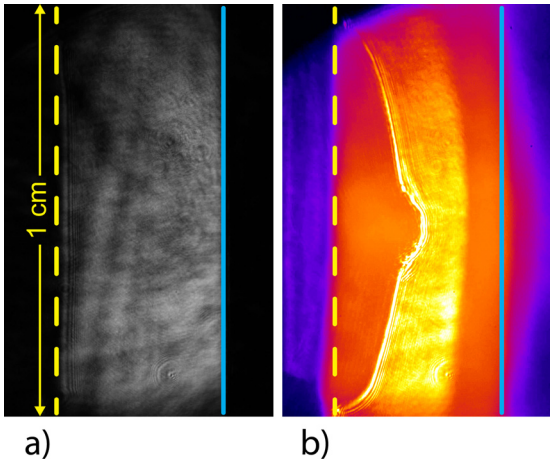

FIG. 9. (Color online) Shadowgraphs with the probe laser parallel to foil current (i.e., along the y-direction in Fig. 2): (a) pre-shot and (b) 190 ns, 0.6 MA. False color has been added in (b) to aid the eye. MRT anisotropy is apparent by comparing Figs. 4 and 9(b).

The + and − signs refer to the values of g evaluated at $\lambda_m = 1.2$ mm and 0.8 mm, respectively. The direct measurements of the acceleration by Zier[15] are shown in Table II. Except for the large offset right side case, Eq. (5) gives an acceleration which is about a factor of 2 less than that from Table II. In other words, the substantial variations in the acceleration that are measured directly (Table II) should have given much larger variations in the experimentally measured growth rates. Perhaps, these large accelerations drove the MRT to the nonlinear stage much earlier so that they render the linear theory of MRT inapplicable, except for the large offset right side case. Note that Eq. (5) is in fact consistent with the *trend* displayed in Table II: the acceleration should be the highest for large offset left side, the lowest for large offset right side, and somewhere in between for small offset either side.

The data presented in Figs. 4–8 were obtained from laser probes directed perpendicular to the foil current flow (i.e., in the z-direction in Fig. 2). Recent modifications allowed for an additional optical path in the direction parallel to foil current flow (i.e., in the y-direction in Fig. 2). A typical image of the latter for a small offset foil is shown in Fig. 9. Only one side of the expanding foil is visible due to hardware constraints, but similar features are expected on the other side due to symmetry. Fig. 9 shows a characteristic "bump" in the center of the foil in the y-direction, which is consistent with features observed by Hu and Kusse[18] and Bland *et al.*[19] caused by merging plasma streams in linear wire arrays. Comparing Fig. 9(b) and Fig. 4, the anisotropy of MRT is apparent. Future work will focus on the correlation between MRT development in the directions parallel and perpendicular to current.

IV. CONCLUDING REMARKS

This paper presents experimental results of MRT on ablation plasmas from aluminum foils of 400 nm thickness, using a MA linear transformer driver. It is found that the thin foil was ablated into a plasma slab of substantially larger width, leading to a very small MRT feedthrough factor between the two edges of this plasma slab. MRT developed on both edges of the plasma slab with comparable growth rates, regardless of the initial offset position of the foil. These growth rates were qualitatively interpreted using a simple analytic model. Anisotropy of MRT was also observed from laser probes directed parallel and perpendicular to the foil currents.

ACKNOWLEDGMENTS

We acknowledge fruitful discussions with Steve Slutz, Edmund Yu, Sasha Velikovich, Bruce Kusse, Dimitri Ryutov, and Kyle Peterson. This work was supported by DoE Award number DE-SC0002590, NSF Grant number PHY 0903340, and by US DoE through Sandia National Labs award numbers 240985 and 76822 to the University of Michigan. Sandia is a multiprogram laboratory operated by Sandia Corporation, a Lockheed Martin Company, for the US DoE's NNSA under Contract DE-AC04-94AL85000. J. C. Zier and S. G. Patel were supported by NPSC fellowships through Sandia National Laboratories, M. R. Gomez was supported by a SSGF fellowship through NNSA, and D. M. French was supported by a NDSEG fellowship.

[1]D. B. Sinars, S. A. Slutz, M. C. Herrmann, R. D. McBride, M. E. Cuneo, K. J. Peterson, R. A. Vesey, C. Nakhleh, B. E. Blue, K. Killebrew, D. Schroen, K. Tomlinson, A. D. Edens, M. R. Lopez, I. C. Smith, J. Shores, V. Bigman, G. R. Bennett, B. W. Atherton, M. Savage, W. A. Stygar, G. T. Leifeste, and J. L. Porter, Phys. Rev. Lett. **105**, 185001 (2010).
[2]D. B. Sinars, S. A. Slutz, M. C. Herrmann, R. D. McBride, M. E. Cuneo, C. A. Jennings, J. P. Chittenden, A. L. Velikovich, K. J. Peterson, R. A. Vesey, C. Nakhleh, E. M. Waisman, B. E. Blue, K. Killebrew, D. Schroen, K. Tomlinson, A. D. Edens, M. R. Lopez, I. C. Smith, J. Shores, V. Bigman, G. R. Bennett, B. W. Atherton, M. Savage, W. A. Stygar, G. T. Leifeste, and J. L. Porter, Phys. Plasmas **18**, 056301 (2011).
[3]S. A. Slutz, M. C. Herrmann, R. A. Vesey, A. B. Sefkow, D. B. Sinars, D. C. Rovang, K. J. Peterson, and M. E. Cuneo, Phys. Plasmas **17**, 056303 (2010).
[4]R. C. Kirkpatrick, I. R. Lindemuth, and M. S. Ward, Fusion Technol. **27**, 201 (1995); I. R. Lindemuth and R. C. Kirkpatrick, Nucl. Fusion **23**, 263 (1983).
[5]R. E. Sieman, I. R. Lindemuth, and K. F. Schoenberg, Comments Plasma Phys. Controlled Fusion **18**, 363 (1999). Available at http://fusionenergy.lanl.gov/Documents/MTF/Why_MTF/Why-MTF-Comments.html.
[6]I. R. Lindemuth, R. E. Reinovsky, R. E. Chrien, J. M. Christian, C. A. Ekdahl, J. H. Goforth, R. C. Haight, G. Idzorek, N. S. King, R. C. Kirkpatrick, R. E. Larson, G. L. Morgan, B. W. Olinger, H. Oona, P. T. Sheehey, J. S. Shlachter, R. C. Smith, L. R. Veeser, B. J. Warthen, S. M. Younger, V. K. Chernyshev, V. N. Mokhov, A. N. Demin, Y. N. Dolin, S. F. Garanin, V. A. Ivanov, V. P. Korchagin, O. D. Mikhailov, I. V. Morozov, S. V. Pak, E. S. Pavlovskii, N. Y. Seleznev, A. N. Skobelev, G. I. Volkov, and V. A. Yakubov, Phys. Rev. Lett. **75**, 1953 (1995).
[7]T. Intrator, M. Taccetti, D. A. Clark, J. H. Degnan, D. Gale, S. Coffey, J. Garcia, P. Rodriguez, W. Sommars, B. Marshall, F. Wysocki, R. Siemon, R. Faehl, K. Forman, R. Bartlett, T. Cavazos, R. J. Faehl, K. Forman, M. H. Frese, D. Fulton, J. C. Gueits, T. W. Hussey, R. Kirkpatrick, G. F. Kiuttu, F. M. Lehr, J. D. Letterio, I. Lindemuth, W. McCullough, R. Moses, R. E. Peterkin, R. E. Reinovsky, N. F. Roderick, E. L. Ruden, K. F. Schoenberg, D. Scudder, J. Shlachter, and G. A. Wurden, Nucl. Fusion **42**, 211 (2002).
[8]T. Intrator, S. Y. Zhang, J. H. Degnan, I. Furno, C. Grabowski, S. C. Hsu, E. L. Ruden, P. G. Sanchez, J. M. Taccetti, M. Tuszewski, W. J. Waganaar, and G. A. Wurden, Phys. Plasmas **11**, 2580 (2004).
[9]E. G. Harris, Phys. Fluids **5**, 1057 (1962).
[10]M. Kruskal and M. Schwarzschild, Proc. R. Soc. London, Ser. A **223**, 348 (1954).

[11]S. Chandrasekhar, *Hydrodynamic and Hydromagnetic Stability* (Oxford University Press, London, 1961).
[12]D. D. Ryutov, M. S. Derzon, and M. K. Matzen, Rev. Mod. Phys. **72**, 167 (2000).
[13]Y. Y. Lau, J. C. Zier, I. M. Rittersdorf, M. R. Weis, and R. M. Gilgenbach, Phys. Rev. E **83**, 066405 (2011).
[14]Y. Y. Lau, R. M. Gilgenbach, J. C. Zier, D. Chalenski, D. M. French, M. R. Gomez, S. G. Patel, I. M. Rittersdorf, A. Steiner, M. R. Weis, P. Zhang, M. Mazarakis, M. E. Cuneo, and M. Lopez, in *AIP Proceedings of the Dense Z-Pinch* (Biarritz, France) (in press).
[15]J. C. Zier, °Ph.D. dissertation, University of Michigan, Ann Arbor, 2010.
[16]R. M. Gilgenbach, M. R. Gomez, J. Zier, W. W. Tang, D. French, Y. Y. Lau, M. G. Mazarakis, M. E. Cuneo, M. D. Johnson, B. V. Oliver, T. A. Mehlhorn, A. A. Kim, and V. A. Sinebryukhov, "MAIZE: A 1 MA LTD-driven Z-pinch at The University of Michigan," in *7th International Conference on Dense Z-pinches* (Alexandria, Virginia, 2008).
[17]E. Yu and K. Peterson, private communication (2011).
[18]M. Hu and B. R. Kusse, Phys. Plasmas **12**, 102701 (2005).
[19]S. N. Bland, S. V. Lebedev, J. P. Chittenden, D. J. Ampleford, and G. Tang, Phys. Plasmas **11**, 4911 (2004).